ELSEVIER

Journal of Photochemistry and Photobiology A: Chemistry 101 (1996) 233–239

Journal of PHOTOCHEMISTRY AND PHOTOBIOLOGY A: CHEMISTRY

Spectroscopic and morphological studies of 3-(2-benzothiazolyl)-7-hexadecyloxycoumarin assembled in Langmuir–Blodgett films

A.K. Dutta, K. Kamada, K. Ohta *

Photonic Chemistry Section, Department of Optical Materials, Osaka National Research Institute, AIST, 1-8-31 Midorigaoka, Ikeda, Osaka 563, Japan

Received 28 March 1996; accepted 10 June 1996

Abstract

We report the behaviour of 3-(2-benzothiazolyl)-7-hexadecyloxycoumarin (HDBOC) mixed with stearic acid (SA) at the air–water interface. Detailed studies of the surface pressure vs. area per molecule isotherm measurements of mixed films of HDBOC and SA indicate the formation of organized aggregates. Miscibility studies reveal that distinct regions of mixing and demixing exist and are dependent on the molar composition and surface pressure exerted on the mixed film. Spectroscopic studies suggest that the HDBOC molecules are sandwiched between SA chains and form J aggregates. A comparative study of the spectroscopic properties in solution and in Langmuir–Blodgett films suggests differences in the molecular conformation of HDBOC in the two systems.

Keywords: Fluorescence; Fluorescence microscopy; J aggregates; Langmuir–Blodgett films

1. Introduction

Ordered ultrathin Langmuir–Blodgett (LB) monolayers and multilayers of amphiphilic molecules containing various functional groups have been the subject of intense research in recent years [1,2]. Such films are important in the design of future generation optoelectronic and photonic devices [3–6]. In addition, the close resemblance of natural biomembranes to LB films provides a unique platform for studying and mimicking biomolecular reactions in energy-harvesting photosynthetic reaction centres, self-assembled pattern formation and molecular recognition processes [7–12]. The chief advantage of using the LB technique over other methods is that the optical and electronic properties of these films may be tailored with ease. Moreover, LB films belong to a family of systems representing restricted geometries which are of interest. Fluorescent dyes incorporated into such systems provide interesting information on the photophysical properties of the dyes in restricted geometries and the interactions between the dye molecules and the microenvironment, which may lead to a better understanding of the correlation between the photophysical and morphological characteristics of these systems.

LB films are not as perfect as they seem, despite their representation as highly organized molecular assemblies in which the functional groups are specifically oriented and homogeneously distributed. Real LB films rarely satisfy such a description. In addition to defects [13–16], the immiscibility of components and the inhomogeneous distribution of functionalized groups cause the formation of aggregates and crystallites [17–32]. Recent studies have revealed that even amphiphilic molecules form aggregates [20–26]. However, little information is available on the mechanism of their formation, much less a complete theory that quantitatively describes the aggregates in terms of their size and distribution. Although aggregation may be undesirable in some cases, it is extremely important in others, e.g. organized aggregation results in extremely high unidirectional conductivities [33–35] and controls the efficiency of fundamental processes, such as energy and electron transfer reactions in real photosynthetic reaction centres [36,37].

In an effort to understand better the photophysical and aggregated properties of dyes in LB films, we have chosen 3-(2-benzothiazolyl)-7-hexadecyloxycoumarin (HDBOC) for our study. There are several reasons for this. HDBOC is a coumarin-based dye which exhibits intense fluorescence in the blue–green region of the visible spectrum, in addition to unique properties such as intense lasing capabilities, low self-quenching, high non-linear optical (NLO) coefficients, pronounced twisted intramolecular charge transfer (TICT) effects and extreme sensitivity to the local environment [38–41].

* Corresponding author. Tel.: 81 727 51 9523; fax: 81 727 51 9628.

PII S1010-6030(96)04429-2

In this work, we report the behaviour of HDBOC mixed with stearic acid (SA) at the air–water interface at different mixture compositions. Detailed studies of the surface pressure vs. area per molecule isotherms of the mixed films at the air–water interface reveal concentration- and pressure-dependent mixing–demixing of the components. Spectroscopic studies reveal the formation of J aggregates, and polarization studies confirm the specific orientation of the HDBOC molecules in LB films. Detailed studies suggest that the molecular conformations of HDBOC in solution and in LB films are different.

2. Experimental details

HDBOC was purchased from Lambda Chemical Company, Switzerland and was used as received. Prior to use, the purity of the samples was checked by thin layer chromatography. SA was obtained from Sigma Chemical Company and was used as received. All solvents were of spectroscopic grade and were used as received from Cica-Merck, Japan. The behaviour of the dye mixed with SA was studied at the air–water interface in a commercially available LB trough (Lauda MGW-Filmwaage) obtained from Lauda Inc., Germany. Deionized water, obtained by purifying double distilled water through a Diastill water purification system, was used as the subphase. The pH of the subphase was 6.4 in equilibrium with atmospheric carbon dioxide and the temperature of the subphase was maintained constant at 20 °C by a closed cycle refrigerating system provided by Lauda Inc. The surface pressure was measured by a piezoelectric sensor with an accuracy of 0.1 mN m^{-1}, and constant surface pressure was maintained by the movable barrier which was interfaced to the piezoelectric sensor through a computer.

Fluorescent grade quartz plates were cleaned by chromic trioxide and subsequently with boiling nitric acid to remove all traces of organic matter and repeatedly washed with water. The slides were then sonicated in spectroscopic grade chloroform for about 15 min, dried and stored in dust-free vacuum chambers until use.

Absorption spectra in solution and in LB films were recorded on a Shimadzu 2010 UVPC absorption spectrophotometer and emission spectra were recorded on a Hitachi 3010 fluorometer. Fluorescence emission from the LB films was collected by placing the LB films in special holders such that they were inclined at an angle of 45° to both the source and detector. Polarized emission was recorded using polymer-based polarizing sheets which were transparent in the 350–800 nm region in the path of incident and emission beams. Fluorescence micrographs were obtained on a commercially available BioRad confocal scanning fluorescence microscope and the photographs were recorded by a Nikon camera attached to the microscope. Excitation of the dye molecules in the LB films was achieved by a helium–cadmium laser (5 W) at 420 nm.

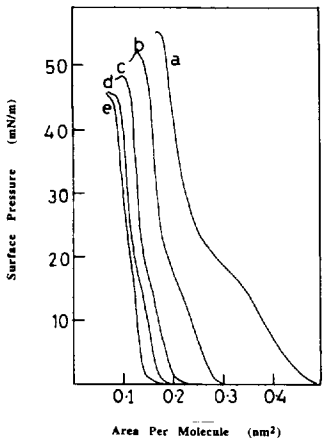

Fig. 1. Surface pressure vs. area per molecule isotherms of HDBOC mixed with SA at different mole fractions of HDBOC in the mixture: (a) 0; (b) 0.28; (c) 0.49; (d) 0.79; (e) 1.00.

3. Results and discussion

3.1. Surface pressure vs. area per molecule isotherms at the air–water interface

When a small volume (100 μl) of a solution of pure HDBOC (5×10^{-3} M) in chloroform is spread at the air–water interface and compressed slowly, after allowing sufficient time for the volatile solvent to evaporate, the *Π–A* isotherm obtained typically represents the isotherm of non-amphiphilic molecules which form clusters and are pushed together at the air–water interface [1,2]. Although the pure and mixed films of HDBOC formed at the air–water interface are extremely stable with time, as obtained from a plot of the area per molecule vs. time at constant surface pressure (figure not shown), all attempts to transfer the films of pure HDBOC from the air–water interface onto quartz substrates failed. However, mixing HDBOC with SA results in the formation of uniform, homogeneous LB films which can be readily transferred onto solid supports with a high transfer ratio of about 0.98.

Fig. 1 shows the surface pressure vs. area per molecule isotherms of pure and mixed films of HDBOC with SA. The low area per molecule of pure HDBOC suggests that the HDBOC molecule does not lay flat at the air–water interface, but probably stands on its edge. The average area per molecule decreases with increasing concentration of HDBOC and attains magnitudes much lower than the area occupied by pure SA. These results suggest that the molecules are either squeezed in between SA chains, so as not to occupy area at the air–water interface, or precipitated in the subphase. To confirm whether or not HDBOC moieties are precipitated into the bulk of the subphase, a large number of small aliquots of water drawn from the subphase were examined spectroscopically in a fluorometer. The failure to detect the characteristic fluorescence emission of HDBOC confirmed that the dye molecules were not precipitated into the bulk of the subphase. On the other hand, the increase in absorbance and

emission with increasing concentration of HDBOC (figure not shown) suggests the incorporation of HDBOC molecules in LB films. A reasonable possibility seems to be that the HDBOC molecules are squeezed in between the SA chains so as not to occupy any area at the air–water interface. Polarization studies, discussed in Section 3.3, confirm that the HDBOC molecule stands on its edge and is sandwiched in between the SA chains, such that the S_1–S_0 transition dipole moment has its maximum component parallel to the dipping direction.

The immiscibility of the components is one of the principal causes of aggregation. Although non-amphiphilic molecules mixed with fatty acids separate in phase owing to the large dissimilarity between their physical and chemical properties, amphiphilic molecules and fatty acids form partially miscible systems. Extensive studies [20–36] have demonstrated that the extent of miscibility or immiscibility depends on several factors, such as the molar composition, temperature and surface pressure. Brewster angle microscopy (BAM) [33–35] and fluorescence microscopy [36] provide unique methodologies for visualizing the formation of aggregates and phase separation processes. A simple and reliable estimate of the miscibility of the components in a mixture and the nature of interaction between the components at the air–water interface may also be obtained from the excess average area per molecule vs. the molar concentration of the mixed films at different surface pressures. In an ideal system of molecules, where all possible interactions between the molecules are assumed to be absent, the average area per molecule is given by the relation [37–40]

$$A_{12} = N_1A_1 + N_2A_2$$

where N_1, N_2 and A_1, A_2 correspond to the mole fractions and areas per molecule of the individual components of the mixture and A_{12} is the average area per molecule of the mixture. Deviations from the ideality curve in real systems originate from the existence of interactions between the components in the mixture. While a repulsive [41–43] interaction between components causes a positive deviation from the ideality curve, a negative deviation suggests an attractive [44–46] interaction between the components. Deviations from the ideality curve suggest immiscibility of the components which may be accounted for in terms of the specific orientation, organization and packing of the components in a monolayer.

Fig. 2 shows a plot of the excess average area per molecule (ΔA) vs. the molar concentration of HDBOC in a mixed film of HDBOC and SA at different surface pressures. The excess average surface area is the difference between the observed average area and the sum of the areas of the pure components, and is mathematically expressed as $\Delta A = [A_{12} - (N_1A_1 + N_2A_2)]$. The line corresponding to zero difference ($\Delta A = 0$) suggests ideal mixing, whereas deviations from the zero line suggest demixing of the components. A close examination of Fig. 2 reveals that the extent of mixing and demixing is both concentration and pressure dependent. The deviation of the

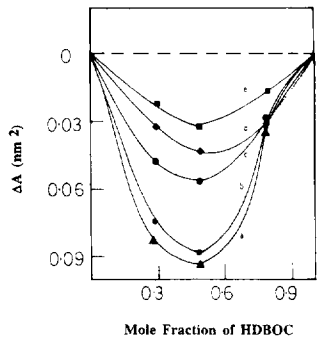

Fig. 2. Plot of the excess average area per molecule (ΔA) vs. the mole fraction of HDBOC in a mixture of HDBOC and SA at different surface pressures: (a) 5 mN m^{-1}; (b) 10 mN m^{-1}; (c) 20 mN m^{-1}; (d) 25 mN m^{-1}; (e) 30 mN m^{-1}.

excess area vs. mole fraction curve from the ideality curve is larger at low surface pressures than at high surface pressures. This implies that, at low surface pressure, the components of the mixture tend to demix more than at high pressures. Another interesting feature observed in this study is that, although maximum demixing is observed at 0.5 mole fraction of the mixture at all surface pressures, a larger miscibility is observed at concentrations higher or lower than this value.

At the air–water interface, in addition to a strong interaction between the molecules and the water surface which tends to orient the chromophores in a specific manner, other predominant interactions are the SA–SA, HDBOC–HDBOC and SA–HDBOC interactions; these contribute strongly towards the mixing–demixing process at the air–water interface, which also determines the spatial distribution of the components in the film and the formation of crystallites. Interactions between similar species, namely SA–SA and HDBOC–HDBOC, are much stronger than SA–HDBOC interactions, which tends to promote demixing processes resulting in the formation of domains of pure components. As the strength of interaction between the molecules is dependent on the distance of separation between the molecules, the extent of mixing–demixing is expected to depend on the molar composition of the mixture as well as the surface pressure. Moreover, the observation that maximum demixing occurs at a molar composition of 0.5, independent of the surface pressure, confirms that the SA–SA and HDBOC–HDBOC interactions prevail over the SA–HDBOC interactions. In addition, the larger miscibility observed at higher surface pressures, independent of the concentration, indicates that with increasing pressure the molecules are forced into close proximity with each other enhancing the attractive interaction between the components and hence the miscibility.

Concentration-dependent studies have revealed that, at low mole fractions of HDBOC in the mixture, the components tend to be completely miscible independent of the surface pressure. One plausible reason may be that, at low concentrations of HDBOC, SA molecules offer a microphase in which the dye molecules are readily accommodated. Fluorescence micrographs discussed in Section 3.2 confirm the high miscibility of the dye molecules in the SA microphase,

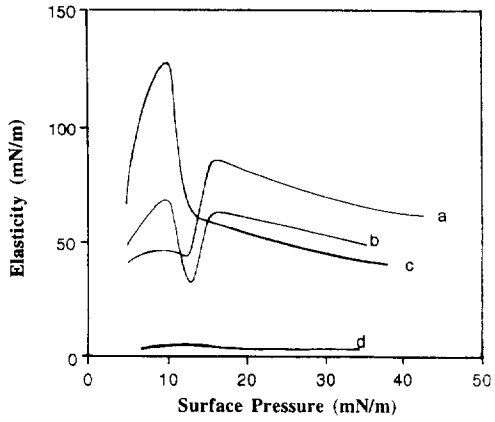

Fig. 3. Plot of the modulus of elasticity of the mixed film of HDBOC and SA vs. the surface pressure at different mole fractions of HDBOC in the mixture: (a) 0.28; (b) 0.49; (c) 0.79; (d) 1.00.

forming almost homogeneous mixed phases in the LB films at low concentrations of HDBOC. However, at higher concentrations, demixing results in phase separation of the components, forming microcrystallites and domains of pure dye molecules, the existence of which is confirmed by fluorescence microscopy. Similar results have been observed in the mixed system of ω-anthrylalkanoic and alkanoic acids with the formation of crystallites confirmed by BAM studies [47]. In this context, it may be pointed out that the above-mentioned observed effects are not due to specific interactions between the functional group and the neighbouring fatty acid, but are a general feature of mixed systems where, as mentioned previously, the mixing–demixing process is controlled by the interaction between the molecules in the mixture. Detailed thermodynamic studies by Dorfler et al. [48] have demonstrated that, while complete miscibility of pure alkanoic acids is observed when the chain lengths of the components in the mixture differ by a maximum of four CH_2 units, phase separation results when this limit is exceeded.

Fig. 3 shows a plot of the elasticity of the mixed films of HDBOC and SA at different molar compositions vs. the surface pressure applied at the air–water interface. The modulus of elasticity is obtained from the *Π–A* isotherms using the mathematical relation [49]

$$K = -A(\partial \Pi / \partial A)_A = \text{constant}$$

These dynamic elasticity measurements provide much information on the mechanical properties of the mixed film at the air–water interface during compression. As is evident from the figure, the dependence of elasticity on the surface pressure is complex. The sharp changes observed at low surface pressure possibly correspond to the different phase transitions undergone by the mixed film during compression. With increasing surface pressure, the coefficient of elasticity decreases continuously and becomes almost constant, indicating that a solid condensed phase has been attained. This seems justified in view of the fact that, with increasing surface pressure, the intramolecular interactions between the components increase resulting in the formation of incompressible solid crystallites. These results are also consistent with those of *Π–A* isotherms. Identical observations have been made by Alekseev et al. [50] for mixed films of myristic acid and an amphiphilic aminocoumarin derivative. Perhaps the most outstanding feature observed in this study is the behaviour of pure HDBOC at the air–water interface; the elasticity vs. surface pressure curve is a straight line almost parallel to the surface pressure axis, which implies the formation of incompressible solid crystalline domains of HDBOC at the air–water interface independent of the surface pressure. These features readily confirm the low area per molecule of pure HDBOC and the existence of intense hydrophobic interactions between the HDBOC and water molecules and strong van der Waals' interactions which contribute to the formation of crystallites.

3.2. Morphological aspects of the LB films of HDBOC mixed with SA studied by scanning confocal fluorescence microscopy

Fig. 4 shows the fluorescence micrographs of mixed LB films of HDBOC and SA at different molar compositions at a constant surface pressure of 25 mN m^{-1}. Fig. 4(a) and (b) correspond to the fluorescence micrographs of HDBOC at molar concentrations of 0.05 and 0.1 in the mixed film. The homogeneous, bright green islands observed correspond to the fluorescence from the HDBOC dye dispersed in the SA microphase, whereas the dark regions correspond to non-fluorescent SA. The homogeneous appearance of the islands and the lack of granular and crystalline structures indicate that the HDBOC molecules are probably solubilized in the SA matrix; this is confirmed by the excess surface area vs. mole fraction curves discussed in Section 3.1. With increasing molar concentration of HDBOC in the mixed film, in addition to the overall island structure, bright spots appear in a variety of colours, shapes and sizes as shown in Fig. 4(c). Close examination of these structures reveals that the spots correspond to microcrystallites. It should be noted that Kopelman and coworkers [51,52] have reported different coloured crystallites of perylene and tetracene doped in a poly(methyl methacrylate) (PMMA) matrix, and detailed studies have revealed that the colours depend on the size of the crystallites. Furthermore, it has been observed that, with increasing dye concentration, the average size of the crystallites increases, although an assortment of different sized clusters are available. Fig. 4(d) shows a magnified view of a large cluster of HDBOC formed in the LB film at a high molar composition of 0.25, which confirms the extensive demixing of the components in the mixed film. Indeed, these results are consistent in view of the completely different physical and chemical characteristics of SA and HDBOC, discussed earlier. In addition to the visual evidence of the phase separation of the components in the LB films, as revealed by fluorescence microscopic studies, spectroscopic studies (discussed in Section 3.3) confirm that the molecules forming the crystallites

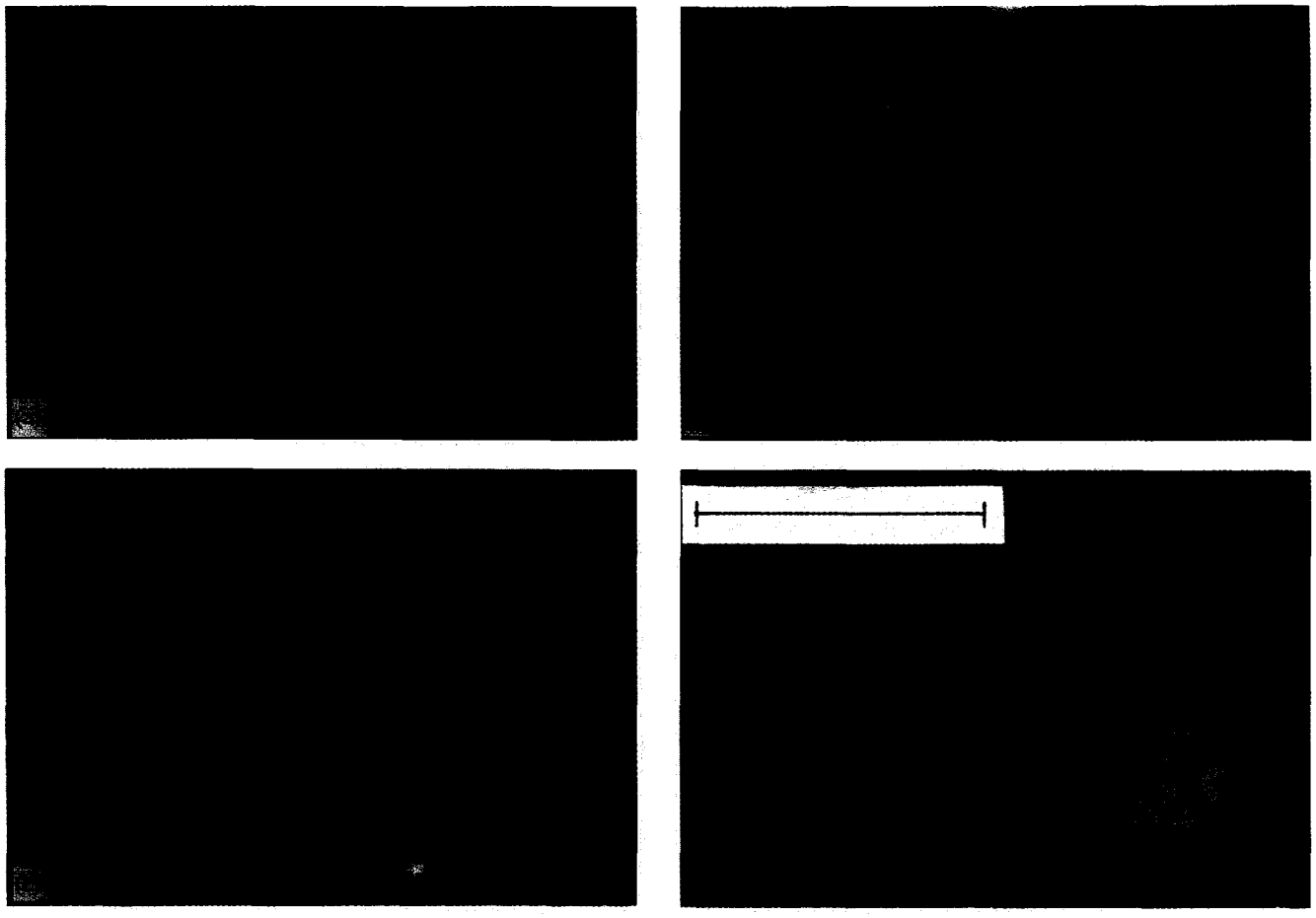

Fig. 4. Fluorescence micrographs of mixed films of HDBOC and SA deposited on quartz slides at a constant surface pressure of 25 mN m^{-1} at different mole fractions of HDBOC in the mixture: (a) 0.05; (b) 0.1; (c) 0.2; (d) 0.25. The bar on the photograph represents 20 μm.

are not randomly oriented within the crystallite, but are highly oriented and organized.

3.3. Spectroscopic study of HDBOC in solution and in mixed LB films with SA

Fig. 5 shows the absorption spectra of HDBOC in carbon tetrachloride and in mixed LB films with SA. The solution absorption spectrum shows bands at 380 and 395 nm, with the 0–0 band at 420 nm. The LB film absorption spectrum shows bands at 395 and 415 nm, with the 0–0 band at 440 nm. The broadening and large red shift of the absorption bands by about 20 nm suggest aggregation and strong dipole–dipole interaction between the moieties in the aggregates.

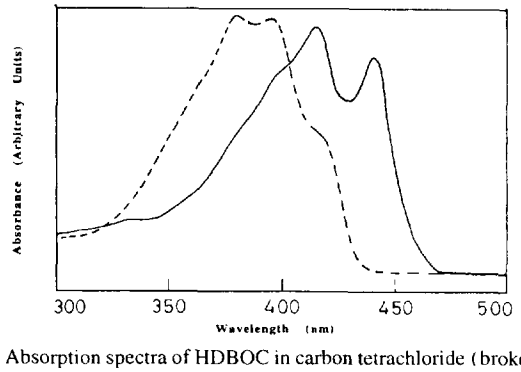

Fig. 5. Absorption spectra of HDBOC in carbon tetrachloride (broken line) and in an LB film with an HDBOC : SA molar ratio of 1 : 10 (10 layers) (full line).

According to the exciton theory proposed by Kasha and coworkers [53–55], dipole–dipole interactions lead to the formation of an exciton band which is located either above or below the monomeric band, and the shift is determined by the relation

$$\Delta\nu = (2/hc)([N-1]/N)\mu^2/r^3(1-3\cos^2\Theta)$$

where $\Delta\nu$ is the shift of the exciton band, N is the number of monomers in the aggregates, μ is the dipole moment, Θ is the angle between the dipoles and r is the vector joining the centres of the dipoles. From the above mathematical relation, it is clear that $0° < \Theta < 54.7°$ causes a red shift, and the corresponding aggregates are referred to as J aggregates [54–56]; for $54.7° < \Theta < 90°$, a blue shift of the bands occurs and the corresponding aggregates are referred to as H aggregates [56–58]. It is evident from the exciton coupling theory that the aggregates formed in the LB films are very probably J aggregates, unlike the H aggregates of 7-aminocoumarin. Furthermore, Alekseev et al. [50] reported large changes in the absorption and emission band positions and shapes depending on the type of deposition and surface pressure at which LB deposition was achieved. Such changes have been

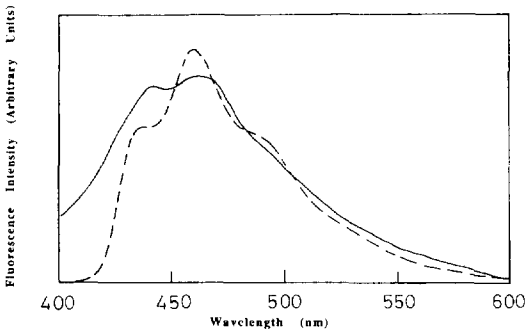

Fig. 6. Emission spectra of HDBOC in carbon tetrachloride (broken line) and in an LB film with an HDBOC : SA molar ratio of 1 : 10 (10 layers) (full line) (λ_{exc} = 400 nm).

interpreted to arise from the interaction between the interlayers. However, no such changes were observed in this case for HDBOC.

Fig. 6 shows the emission spectra of HDBOC in carbon tetrachloride and in mixed LB films with SA. In solution, the emission bands are located at 437, 459 and 487 nm, whereas in the LB films they are located at 440 and 465 nm. Although the 0–0 bands of absorption and emission for HDBOC in carbon tetrachloride are separated by about 17 nm, there is almost no shift between the 0–0 bands for absorption and emission in LB films. Although these results do not seem to be readily explicable, one possible explanation may be that the molecular conformations of HDBOC in solution and in LB films are different. Estimates of the polarity (Δf) obtained from the relation

$$\Delta f = (\epsilon - 1)/(2\epsilon + 1) - (n^2 - 1)/(2n^2 + 1)$$

show that Δf for SA is 0.008, whereas Δf for carbon tetrachloride is 0.011. The refractive index (n) and dielectric constant (ϵ) values used for the calculations were obtained from Ref. [59]. A change in molecular conformation of HDBOC may originate from the different polarity in the two systems. One possibility may be the rotation of the benzothiazolyl group about the coumarin group; this is justified in view of the fact that similar large, polarity-dependent spectroscopic changes have been reported in the literature and have been attributed to TICT effects [60].

Polarization studies of LB films of HDBOC mixed with SA reveal that the fluorescence intensity of VV polarization is larger than that of VH polarization, where VV and VH polarizations correspond to the axis of polarization directed parallel or perpendicular to the dipping direction. These results suggest that the long axis of the molecule, corresponding to the S_1–S_0 transition [61], has a larger component parallel to the dipping direction of the substrate than perpendicular to it. However, a precise determination of the orientation of the moieties is not possible by this method. An estimate of the polarization anisotropy parameter (r) obtained from the polarized fluorescence spectra, using the relation $r = (I_{VV} - I_{VH})/(I_{VV} + 2I_{VH})$, yields $r = 0.4$, corresponding to the 0–0 band of fluorescence. Using the auxiliary relation $r = 0.2(3\cos^2 \Phi - 1)$, where Φ is the angle between the directions of the transition moments corresponding to the absorption and emission dipole moments [62], yields $\Phi = 0°$, which indicates that absorption and emission occur from the same electronic state (a general feature of most rigid aromatic hydrocarbons). These results are again sharply in contrast with those obtained for rigid amphiphilic 7-aminocoumarins assembled in LB films, where Φ is estimated to be about 63°, suggesting that the absorption and emission occur from different states. Although photons are absorbed by the monomers, efficient energy transfer from the monomers to the aggregates occurs, resulting in emission from the lowest excited singlet state, corresponding to the aggregates of aminocoumarin [63].

4. Conclusions

Our preliminary studies report the formation of highly fluorescent LB films of HDBOC mixed with SA. Detailed studies of the surface pressure vs. area per molecule isotherms at the air–water interface indicate that the HDBOC molecules stand almost vertically at the air–water interface and are sandwiched between SA chains. Plots of the excess area per molecule vs. mole fraction of the mixed films of HDBOC and SA show large deviation from the ideality curve indicating immiscibility of the components of the mixture. Close examination of these curves reveals distinct mixing–demixing zones which are dependent on the molar composition and surface pressure of the mixed system. Fluorescence microscopic studies of the films confirm the partial miscibility at low mole fractions of the dye in the mixture and the formation of clusters due to immiscibility of the components at larger dye concentrations. Elasticity measurements of the mixed films of HDBOC and SA at the air–water interface show a sharp decrease at higher surface pressures. This indicates the formation of incompressible microcrystalline clusters formed at the air–water interface, explained by the dissimilarity between the physical and chemical properties of SA and HDBOC. Spectroscopic studies confirm the formation of highly organized J aggregates of HDBOC in the LB films. Polarization studies suggest that the HDBOC molecules stand with their long axes almost parallel to the normal of the substrate and are stacked as J aggregates. Moreover, the separation of the 0–0 bands of absorption and emission by about 17 nm in solution and the lack of separation in LB films suggest differences in the molecular conformations of HDBOC in solution and in LB films.

Acknowledgements

The authors wish to thank Dr. Soichi Otsuki and Dr. Takashi Taguchi (Department of Organic Materials, Osaka National Research Institute (ONRI)) and Dr. Masanori Ando (Department of Energy and the Environment, ONRI) for providing laboratory facilities. A.K.D. wishes to thank

the Science and Technology Agency of Japan for a fellowship.

References

[1] A. Ulman, *An Introduction to Ultrathin Organic Films*, Academic Press, San Diego, CA, 1991.
[2] R.H. Tredgold, *Order in Thin Organic Films*, Cambridge University Press, Cambridge, 1994.
[3] P. Stroeve and E. Franses, *Molecular Engineering of Ultrathin Polymeric Films*, Elsevier Applied Science, Crown House, Essex, 1987.
[4] P. Stroeve and A.C. Balazs (eds.), *Macromolecular Assemblies in Polymeric Systems*, American Chemical Society, Washington DC, 1992.
[5] J. Messier, F. Kajzar and P. Prasad, *Organic Molecules for Non-Linear Optics and Photonics*, Kluwer Academic Publishers, 1991.
[6] G. Berkovic and Y.R. Shen, in P.N. Prasad and D.R. Ulrich (eds.), *Non-Linear Optical and Electroactive Polymers*, Plenum, New York, 1988.
[7] H. Kuhn, in H. Gerischer and J.J. Katz (eds.), *Light Induced Charge Separation in Biology and Chemistry*, Dahlem Konferenzen, Berlin, 1979, pp. 151–169.
[8] K. Kalyansundaram, *Photochemistry in Microheterogeneous Systems*, Academic Press, New York, 1988.
[9] J. Sagiv, *J. Am. Chem. Soc., 102* (1980) 92.
[10] J.D. Swalen, D.L. Allara, J.D. Andrade, E.A. Chandross, S. Garoff, J. Israelachvilli, T.J. McCarthy, R. Murray, R.F. Pease, J.F. Rabolt, K.J. Wynne and H. Yu, *Langmuir, 3* (1987) 932.
[11] G.P. Lopez, M.W. Albers, S.L. Schreiber, R. Caroll, E. Peralta and G.M. Whitesides, *J. Am. Chem. Soc., 115* (1993) 5877.
[12] G.P. Lopez, H.A. Biebuyck, C.D. Frisbie and G.M. Whitesides, *Science, 260* (1993) 647.
[13] D.K. Schwartz, R. Viswanathan and J.A.N. Zasadzinski, *J. Phys. Chem., 96* (1992) 10 444.
[14] D.K. Schwartz, J. Garneas, R. Viswanathan and J.A.N. Zasadzinski, *Science, 257* (1992) 508.
[15] J. Garneas, D.K. Schwartz, R. Viswanathan and J.A.N. Zasadzinski, *Nature, 357* (1992) 54.
[16] A. Schaper, L. Woltham, D. Mobius and T.M. Jovin, *Langmuir, 9* (1993) 2178.
[17] E.E. Jelly, *Nature, 138* (1936) 1009.
[18] G. Schiebe, *Angew. Chem., 49* (1936) 563.
[19] H. Kuhn, D. Mobius and H. Bucher, in A. Weissberger and B.W. Rositer (eds.), *Techniques of Chemistry*, Vol. 1, Wiley, New York, 1973, Part 3B.
[20] H. Kuhn and D. Mobius, *Angew. Chem., 83* (1971) 672.
[21] H. Kuhn and D. Mobius, *Angew. Chem. Int. Ed. Engl., 10* (1972) 620.
[22] I. Furman, H.C. Geiger, D.G. Whitten, T.L. Penner and A. Ulman, *Langmuir, 10* (1994) 837.
[23] H. Chen, W.G. Herkstroeker, J. Perlstein, K.Y. Law and D.G. Whitten, *J. Phys. Chem., 98* (1994) 5138.
[24] S. Kirstein, R. Steitz, R. Garbella and H. Mohwald, *J. Chem. Phys., 103* (1995) 818, 826.
[25] B.R. Heywood and S. Mann, *Chem. Mater., 6* (1994) 311.
[26] M. Gavish, R. Popovitz-Biro, M. Lahav and L. Leiserowicz, *Science, 250* (1990) 973.
[27] B.R. Heywood and S. Mann, *Adv. Mater., 6* (1994) 9.
[28] A.K. Dutta, T.N. Misra and A.J. Pal, *J. Phys. Chem., 98* (1994) 4365.
[29] A.K. Dutta, T.N. Misra and A.J. Pal, *J. Phys. Chem., 98* (1994) 12 844.
[30] A.K. Dutta, *J. Phys. Chem., 99* (1995) 14 758.
[31] A.K. Dutta, T.N. Misra and A.J. Pal, *Langmuir, 12* (1996) 459.
[32] J.G. Warren, J.P. Cresswell, M.C. Petty, J.P. Lloyd, A. Vitukhnovsky and M.I. Sluch, *Thin Solid Films, 179* (1989) 515.
[33] G.L. Gaines, Jr., *J. Colloid Interface Sci., 85* (1982) 16.
[34] G.L. Gaines, Jr., *Insoluble Monolayers at the Liquid–Gas Interface*, Interscience, New York, 1966.
[35] A.W. Adamson, *Physical Chemistry of Surfaces*, Wiley-Interscience, New York, 1990.
[36] P. Pal, A.K. Dutta, T.N. Misra and A.J. Pal, *Langmuir, 10* (1994) 2339.
[37] R.E. Pagano and N.L. Gershfeld, *J. Phys. Chem., 76* (1972) 1238.
[38] D. Honig and D. Mobius, *J. Phys. Chem., 95* (1991) 4590.
[39] S. Siegel, D. Honig, D. Volhardt and D. Mobius, *J. Phys. Chem., 96* (1992) 8157.
[40] S. Kirstein and H. Mohwald, *Chem. Phys. Lett., 189* (1992) 408.
[41] R.M. Weiss and M. McConell, *Nature, 310* (1984) 47.
[42] M.A. Alsina, C. Mesters, G. Valemia, J.M. Garcia-Anton and F. Reig, *Colloid Surf.* (1988/1989) 151.
[43] J. Israelavchvili, *Intermolecular and Surface Forces*, Academic Press, New York, 1994.
[44] A. Gilardoni, E. Margheri and G. Gabrielli, *Colloid Surf., 68* (1992) 235.
[45] F. Bonosi, E. Margheri and G. Gabrielli, *Colloid Surf., 65* (1992) 287.
[46] J.G. Petrov, D. Mobius and A. Angelova, *Langmuir, 8* (1992) 201.
[47] A. Angelova, M. Van der Auweraer, R. Ionov, D. Vollhardt and F.C. DeSchryver, *Langmuir. 11* (1995) 3167.
[48] H.D. Dorfler, C. Koth and W. Rettig, *Langmuir, 11* (1995) 4803.
[49] J.T. Davies and E.K. Rideal, in *Interfacial Phenomena*, Academic Press, 1968, p. 265.
[50] A. Alekseev, J. Peltonen and V. Savransky, *Thin Solid Films, 247* (1994) 226.
[51] S.K. Kook and R. Kopelman, *J. Phys. Chem., 96* (1992) 10 672.
[52] W. Tan, D. Birnbaum, C. Harris, R. Merlin, B. Orr, Z.-Y. Shi, S. Smith, B.A. Thorsrud and R. Kopelman, in H. Masuhara, F.C. DeSchryver, N. Kitamura and N. Tamai (eds.), *Microchemistry, Spectroscopy and Chemistry in Small Domains*, North-Holland, 1994.
[53] M. Kasha, H.R. Rawls and M.A. El-Bayoumi, *Pure Appl. Chem., 11* (1965) 371.
[54] E.G. McRae and M. Kasha, in L. Augenstein, R. Mason and B. Rosenberg (eds.), *Physical Processes in Radiation Biology*, Academic Press, New York, 1964, p. 23.
[55] E.G. McRae and M. Kasha, *J. Chem. Phys., 28* (1958) 721.
[56] V. Czikkey, H.D. Forsterling and H. Kuhn, *Chem. Phys. Lett., 6* (1970) 11.
[57] V. Czikkey, H.D. Forsterling and H. Kuhn, *Chem. Phys. Lett., 6* (1970) 207.
[58] D. Mobius, *Adv. Mater., 7* (1995) 437.
[59] R.C. Weast (ed.), *Handbook of Chemistry and Physics*, CRC Press, Boca Raton, FL, 1985–1986.
[60] W. Rettig and A. Klock, *Can. J. Chem., 63* (1984) 1649.
[61] R.F. Kubin and A.N. Fletcher, *Chem. Phys. Lett., 99* (1983) 49.
[62] J.F. Lakowicz, *Principles of Fluorescence Spectroscopy*, Plenum, New York, 1983, Chapter 5.
[63] A.S. Alekseev, T.V. Konforkina, V.V. Savransky, M.F. Kovalenko, A. Jutila and H. Lemmityinen, *Langmuir, 9* (1993) 376.